Parallel Momentum Distributions as a Probe of Halo Wave Functions

J. H. Kelley,[1,2] Sam M. Austin,[1,2] R. A. Kryger,[1] D. J. Morrissey,[1,3] N. A. Orr,[1,*] B. M. Sherrill,[1,2] M. Thoennessen,[1,2] J. S. Winfield,[1] J. A. Winger,[1,†] and B. M. Young[1,2,‡]

[1]*National Superconducting Cyclotron Laboratory, Michigan State University, East Lansing, Michigan 48824*
[2]*Department of Physics and Astronomy, Michigan State University, East Lansing, Michigan 48824*
[3]*Department of Chemistry, Michigan State University, East Lansing, Michigan 48824*
(Received 27 July 1994)

Distributions of the parallel momentum of ^{10}Be fragments from the breakup of 63A MeV ^{11}Be have been measured for ^{9}Be, ^{93}Nb, ^{181}Ta, and ^{238}U targets. The distributions have similar narrow widths with a mean value of 43.6 ± 1.1 MeV/c FWHM, and agree with a theoretical momentum distribution for the valence neutron in ^{11}Be. The breakup mechanisms do not appear to distort the parallel momentum distribution of the ^{10}Be core. These findings support the existence of a one-neutron halo in ^{11}Be and the use of the parallel momenta of the heavy breakup products as a reliable probe of halo neutron momenta.

PACS numbers: 21.10.Gv, 25.70.Mn, 27.20.+n

Recently, the availability of radioactive nuclear beams for the study of nuclei near the drip lines [1] has led to the discovery that some weakly bound, neutron-rich nuclei exhibit an extended valence neutron distribution [2,3], the neutron halo. Understanding these nuclei is important, both for their intrinsic interest and to refine structure models so they can predict better the properties of nuclei far from stability.

Early evidence for halo structures was found in the enhanced interaction cross sections measured for nuclei such as ^{11}Li, ^{11}Be, and ^{14}Be [4,5]. These large cross sections were interpreted as reflecting an extended neutron halo surrounding a normal sized core. For example, the heaviest particle-stable lithium isotope ^{11}Li has been described as a ^{9}Li core surrounded by two neutrons (see, for example, [6,7]). The halo results from quantum mechanical penetration of the wave function of weakly bound valence neutron(s) outside the potential well of the core [8]. Measurements of the energy dependence of the interaction cross sections of ^{11}Be and ^{11}Li [9,10] confirmed the existence of long neutron tails in the density distributions. While the cross section data were consistent with Hartree-Fock calculations, they were not very sensitive to the details of the nuclear wave functions [10] and thus do not provide a rigorous test of the theoretical models.

In principle it is possible to probe the wave function of halo neutron(s) more directly, by measuring the momentum distribution of the fragments resulting from breakup of the halo nucleus. In the Serber model (developed originally for the deuteron) [11], the momentum distribution of the halo neutrons is mirrored directly in the momenta of the core following direct breakup. This Letter describes high resolution measurements of the momenta of ^{10}Be fragments from the breakup of ^{11}Be, made in an attempt to assess the accuracy with which halo neutron momentum distributions can be determined with this approach. Breakup targets ranging from ^{9}Be to ^{238}U were studied to determine whether the observed distributions depend on the breakup mechanism; nuclear (Coulomb) interactions dominate the breakup for light (heavy) targets.

Studies of the distribution of $p_\perp$ (momentum perpendicular to the beam) gave results that depend on the breakup target [12] due to, for example, initial and final state interactions such as deflection in the Coulomb field [13]. The angular distribution of neutrons showed the presence of the halo in ^{11}Be and ^{11}Li clearly, but it was difficult to disentangle the halo effects from the effects of the reaction mechanisms and final state interactions [14–18].

It has been suggested theoretically that the distribution of $p_\parallel$ (momentum parallel to the beam direction) is less perturbed than $p_\perp$ by absorption and other reaction mechanism effects [13]. In a peripheral direct reaction model [19] the $p_\parallel$ distribution of the core fragment is identical to the halo neutron momentum distribution, except in the far tails of the distribution. A first measurement of the $p_\parallel$ distribution of ^{9}Li fragments following the breakup of ^{11}Li using this technique [20] gave results in good agreement with a theoretical prediction for a ^{181}Ta breakup target [21]. However, there was a weak dependence on the breakup target: The $p_\parallel$ distribution width decreased by $(17 \pm 6)\%$ as the target mass increased from ^{9}Be to ^{238}U [22]. Even such a small target dependence casts doubt on the use of $p_\parallel$ distributions to measure the intrinsic momentum distribution of halo neutrons.

However, there is a complication in studies of the breakup of ^{11}Li that may explain the findings of Refs. [20,22]. Because ^{10}Li is not particle stable, the two neutron breakup of ^{11}Li can follow two routes: $^{11}\text{Li} \rightarrow {}^{9}\text{Li} + 2n$ or $^{11}\text{Li} \rightarrow {}^{10}\text{Li} + n$ followed by $^{10}\text{Li} \rightarrow {}^{9}\text{Li} + n$, which may lead to different $p_\parallel$ distributions. If both processes are important for ^{11}Li, as has been suggested [23], the relative probability of the two routes could depend on the nature of the reaction mechanism. This might account for the dependence of the observed width on target and hence the slight inconsistency with the Serber assumptions. The narrow

 0031-9007/95/74(1)/30(4)$06.00

widths observed in fragment momentum distributions from halo nuclei are about one-fifth of the widths observed in the fragmentation of normal tightly bound nuclei (see, for example, [24] and references therein), and therefore may be more strongly affected by these or other reaction details.

To assess the reliability of $p_{\parallel}$ distributions for probing the halo, it is necessary to study a simple, well-characterized nucleus. In particular, it is important to avoid the three-body effects and sequential processes that play a role in the case of ^{11}Li. The ^{11}Be nucleus, whose well-understood ground state is dominated by a $1s_{1/2}$ neutron state [25], meets these requirements. It is weakly bound ($S_n = 504 \pm 6$ keV), has a large reaction cross section, and sequential processes do not contribute to its breakup into ^{10}Be + n. Furthermore, the excitation energy spectrum from the breakup of ^{11}Be on a Pb target has been measured [26] and is dominated by direct Coulomb breakup into continuum states; low lying excited states make no significant contribution to the breakup cross section.

In the present experiment the K1200 cyclotron at the National Superconducting Cyclotron Laboratory provided a 13 particle nA beam of 80A MeV ^{18}O, and a ^{11}Be beam was produced by fragmentation in a 790 mg/cm^2 Be target located at the first object point of the the A1200 fragment separator [27]. The resulting ^{11}Be beam had an intensity of 4300 sec^{-1} and a mean energy of 63.0A MeV ($\Delta E/E = 2\%$). The momentum distribution of ^{10}Be fragments from the breakup of ^{11}Be was measured with the A1200 operated as a 0° energy-loss spectrometer, in the same manner as in Ref. [20]. The total momentum p of fragments was measured. Since the angular acceptance for breakup fragments limits $p_{\perp}$ to less than 100 MeV/c, $p_{\parallel}$ equals p within 0.05%.

The focal plane detectors comprised a pair of two-dimensional position sensitive parallel plate avalanche counters (PPACs), an ion chamber for measuring energy loss (ΔE), and a thick plastic stopping detector for timing information and total energy (E). Momentum distributions were determined from positions measured by the PPACs at the focal plane. Although the ^{11}Be secondary beam component (2.4%) was less intense than the ^{8}Li, ^{10}Be, ^{13}B, and ^{16}C contaminants, the ^{10}Be breakup fragments from ^{11}Be could be uniquely identified by the combination of ΔE and time of flight through the A1200.

The momentum calibration was obtained by scanning a ^{10}Be beam of known rigidity (determined by the first half of the A1200) across the focal plane, and, at the same time, the efficiency for transmission as a function of position at the focal plane was measured. Breakup targets of ^{9}Be, ^{93}Nb, ^{181}Ta, and ^{238}U were located at the second dispersive image plane of the A1200 and were chosen to have nearly equal energy losses. The target thicknesses were determined from the change in position (momentum) of the ^{10}Be beam at the focal plane when a target was inserted. The ^{10}Be fragment momentum resolution at the focal plane of the A1200 was 0.2% FWHM; straggling in the breakup targets increased this to 0.3%.

Figure 1 shows the $p_{\parallel}$ distributions of ^{10}Be fragments from ^{11}Be breakup. The distributions are very similar for all targets. A low momentum tail is observed in the distribution for the ^{181}Ta target, which was measured for a larger range of momentum (5%). Dissipative mechanisms common in fragmentation of normal nuclei at intermediate energies [24] seem the likely cause of the low momentum tail, but we have also examined the possible role of beam contaminants. Only ^{14}B, whose intensity is 25% that of ^{11}Be, could produce ^{10}Be fragments that satisfy the time-of-flight constraints used to generate the spectra in Fig. 1. These fragments would have a mean momenta of approximately 3340 MeV/c (i.e., in the low momentum tail of the distribution) and would be expected to have a broad distribution [28] that would not perturb the narrow distribution associated with the removal of the halo neutron from ^{11}Be.

The widths of the distributions were extracted as follows: The height of the distribution was taken as the average of fits of Gaussian and Lorentzian line shapes to the data. Linear fits were made to the sides of the distributions around the half-height, and the width at half-height was determined from the separation of the lines. Systematic uncertainties, reflecting a dependence on the choice of gates selecting ^{10}Be reaction products, and statistical uncertainties from the fits contribute nearly equally to the uncertainty in width. Small corrections to the data for the system resolution and the transformation into the ^{11}Be rest frame are detailed in Table I, and the resulting widths are summarized in Fig. 2. The results

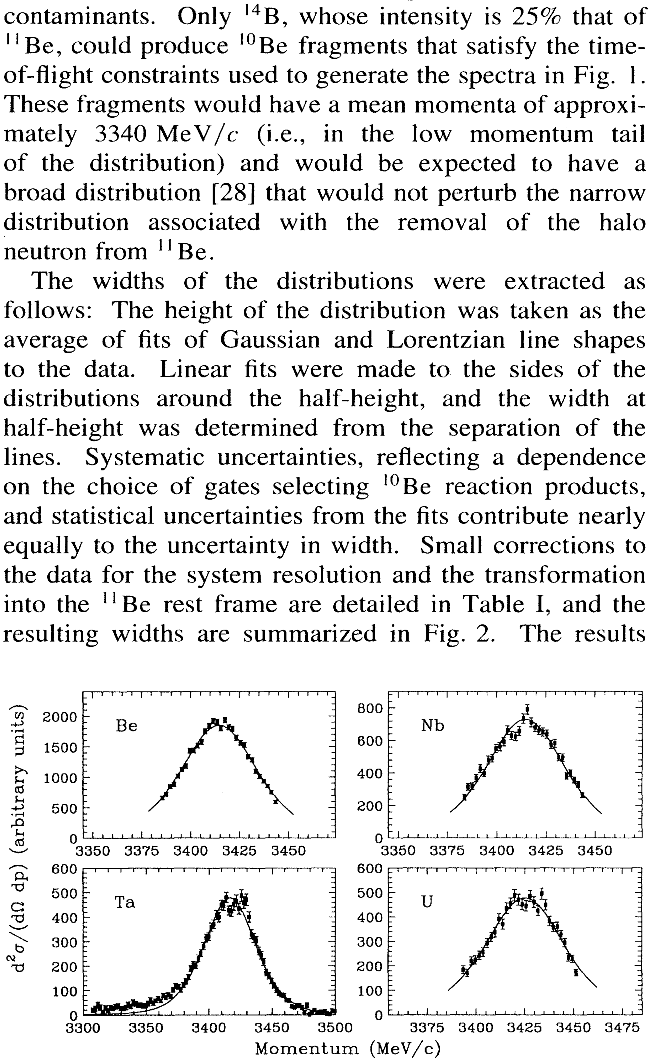

FIG. 1. The $p_{\parallel}$ distributions of ^{10}Be fragments from the breakup of ^{11}Be on various targets. The data are corrected for efficiency of transmission to the focal plane. Additional corrections for the system resolution and the transformation to the ^{11}Be frame are essential to obtain the momentum distribution and are detailed in Table I. The momentum distribution of a $1s_{1/2}$ orbital neutron bound by 500 keV in a Woods-Saxon potential, folded with the experimental effects of resolution and acceptance, and evaluated in the laboratory frame, is compared with the data (solid line).

TABLE I. Widths (uncertainties) of parallel momentum distributions of ^{10}Be fragments following the breakup of ^{11}Be on various targets. All widths are FWHM and the corresponding uncertainties are in parentheses.

Target	Uncorrected (MeV/c)	Efficiency corrected[a] (MeV/c)	System resolution (MeV/c)	Resolution corrected[b] (MeV/c)	^{11}Be rest frame[c] (MeV/c)
^{9}Be	44.5(2.0)	45.3(2.0)	9.3(1.0)	44.3(2.3)	41.6(2.1)
^{93}Nb	48.3(1.9)	50.1(1.9)	11.6(1.0)	48.7(2.2)	45.7(2.0)
^{181}Ta	48.2(1.9)	50.3(2.0)	14.7(1.0)	48.1(2.2)	45.2(2.1)
^{238}U	45.8(2.1)	46.3(2.1)	13.5(1.0)	44.3(2.3)	41.6(2.2)

[a]These correspond to the data displayed in Fig. 1.
[b]Correction made by subtracting in quadrature the system resolution (column 4) from the efficiency corrected widths (column 3).
[c]Results of column 5 expressed in the rest frame of ^{11}Be.

are essentially independent of target and have a weighted average in the ^{11}Be frame of 43.6 ± 1.1 MeV/c FWHM with $\chi_\nu^2 = 1.1$.

Before drawing any final conclusions we consider how the finite acceptance of the A1200 could affect the observed distribution widths. Possible effects are rooted in the connection among the Cartesian components of the momentum density distribution [29]. A Gaussian distribution is separable in Cartesian components, and hence the width of the $p_\parallel$ distribution is unaffected by a finite acceptance. However, for a Lorentzian momentum distribution and the A1200 angular acceptance, $\delta\theta \approx 40$ mrad and $\delta\phi \approx 20$ mrad, we find that the observed width (FWHM) for a Lorentzian with $\Gamma = 50$ MeV/c is reduced by 15%. For more realistic wave functions the effects appear to be smaller. An approximate method, which is accurate to 1% for the width from a Lorentzian distribution [30], shows that the width of the theoretical $p_\parallel$ distribution [31], discussed below, would be decreased by 6% because of acceptance effects in the present experiment.

The narrow widths correspond, via the uncertainty principle, to an extended spatial distribution for the valence neutron of ^{11}Be, and the independence of the widths on the breakup mechanism supports the Serber approach. We take these findings as an indication that the measured width reflects the momentum distribution of the halo neutron. In this spirit we compare the data with the wave function of a $1s_{1/2}$ neutron (which dominates the ^{11}Be ground state wave function) in a Woods-Saxon potential whose depth was adjusted to reproduce the neutron binding energy [31]. When the corresponding spherically symmetric momentum distribution is projected onto one axis the distribution width is 45.4 MeV/c FWHM [31] in the ^{11}Be rest frame. The acceptance correction described above decreases this width to 42.7 MeV/c. The solid line in Fig. 1 is this projected momentum wave function corrected for experimental effects as described in the figure caption. For breakup on heavy targets, the reaction mechanism is expected to modify the momentum distribution at large and small momenta in the ^{11}Be rest frame [18]. However, the distribution shown here, which does not include any reaction mechanism or final state interaction effects, is in good agreement with the data from light and heavy breakup targets.

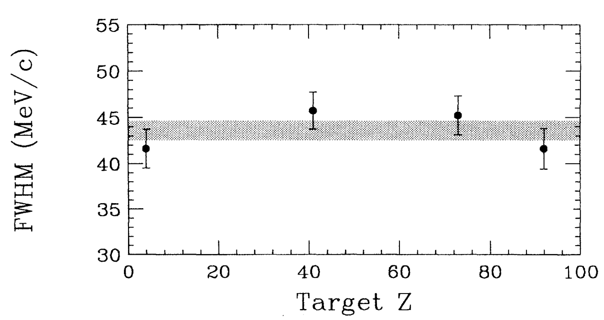

FIG. 2. Summary of the widths of the $p_\parallel$ distributions in the ^{11}Be rest frame. The average width is 43.6 ± 1.1 MeV/c FWHM, shown as a shaded bar. Assuming the shape of the theoretical distribution of Ref. [31], corrections for the acceptance will increase this width to 46.2 MeV/c.

The same Woods-Saxon ground state wave function had been used in a prediction for the angular distribution of neutrons following the breakup of 41A MeV ^{11}Be in a gold target and agrees with the data [15]. The difference in the width of the $p_\parallel$ distribution of ^{10}Be fragments and the width parameter extracted from the neutron angular distribution data ($\Gamma \sim 58 - 63$ MeV/c [15]) may arise from differences in the effects of the reaction mechanism (and in initial and final state interactions) in the $p_\parallel$ and $p_\perp$ directions for halo and core fragments. In contrast to the case for angular distributions, a momentum width can be measured directly from the $p_\parallel$ distribution. As discussed above, this determination should be insensitive to breakup mechanisms.

The root-mean-square radius of this Woods-Saxon wave function, which represents the rms radius for the relative motion of the halo neutron and the core, is 7.2 fm. In the ^{11}Be rest frame this yields a root mean square of 6.5 fm (7.2 fm × 10/11) for the halo neutron and is consistent with the value of 6.4 ± 0.7 fm that is required to reproduce the $E1$ strength observed in the Coulomb breakup of ^{11}Be [26]. Since the observed radius of the ^{10}Be core is 2.30 ± 0.02 fm [5], there is indeed strong evidence for an extended neutron halo in ^{11}Be.

In summary, we have made high resolution measurements of the $p_\parallel$ distribution of ^{10}Be fragments resulting from the breakup of ^{11}Be for a wide range of targets (^{9}Be to ^{238}U). Effects from multiple scattering, energy straggling, and finite acceptance are expected to influence the observed distributions in a similar way, thus allowing an accurate determination of any target dependence. No differences in the width of the distributions were observed, within the uncertainties for individual targets ($\sim$2 MeV/c). Since breakup on light (heavy) targets is dominated by nuclear (Coulomb) interactions, this suggests that any influences of the breakup mechanism or final state interactions are small compared to the width of the $p_{\parallel}$ distribution of ^{10}Be fragments. Taken together with the excellent agreement with the predicted distribution for the ground state valence neutron in ^{11}Be [31], this work supports the existence of a one-neutron halo surrounding a ^{10}Be core in ^{11}Be and the use of the parallel momentum distribution as a probe of the wave functions of halo nuclei.

We are grateful to Henning Esbensen for discussions and unpublished calculations and to Karsten Riisager for helpful comments. This work was supported in part by the National Science Foundation under Grant No. PHY92-14992.

*Present address: LPC, Boulevard du Maréchal Juin, 14050 Caen Cedex, France.

†Present address: Department of Physics and Astronomy, Mississippi State University, Mississippi State, Mississippi 39762.

‡Present address: A.W. Wright Nuclear Structure Laboratory, Yale University, New Haven, Connecticut 06511.

[1] A. C. Mueller and B. M. Sherrill, Annu. Rev. Nucl. Part. Sci. **43**, 529 (1993).
[2] P. G. Hansen, Nucl. Phys. **A553**, 89c (1993).
[3] I. Tanihata, Nucl. Phys. **A522**, 275c (1991).
[4] I. Tanihata *et al.*, Phys. Rev. Lett. **55**, 2676 (1985).
[5] I. Tanihata *et al.*, Phys. Lett. B **206**, 592 (1988).
[6] P. G. Hansen and B. Jonson, Europhys. Lett. **4**, 409 (1987).
[7] M. V. Zhukov *et al.*, Phys. Rep. **231**, 151 (1993).
[8] K. Riisager, A. S. Jensen, and P. Møller, Nucl. Phys. **A548**, 393 (1992).
[9] M. Fukuda *et al.*, Phys. Lett. B **268**, 339 (1991).
[10] I. Tanihata *et al.*, Phys. Lett. B **287**, 307 (1992).
[11] R. Serber, Phys. Rev. **72**, 1008 (1947).
[12] T. Kobayashi *et al.*, Phys. Rev. Lett. **60**, 2599 (1988).
[13] C. A. Bertulani and K. W. McVoy, Phys. Rev. C **46**, 2638 (1992).
[14] R. Anne *et al.*, Phys. Lett. B **250**, 19 (1990).
[15] R. Anne *et al.*, Phys. Lett. B **304**, 55 (1993).
[16] F. Barranco, E. Vigezzi, and R. A. Broglia, Phys. Lett. B **319**, 387 (1993).
[17] P. Banerjee and R. Shyam, Phys. Lett. B **318**, 268 (1993).
[18] R. Anne *et al.*, Nucl. Phys. **A575**, 125 (1994).
[19] H. Sagawa and N. Takigawa, Phys. Rev. C **50**, 985 (1994).
[20] N. A. Orr *et al.*, Phys. Rev. Lett. **69**, 2050 (1992).
[21] H. Esbensen, G. F. Bertsch, and K. Ieki, Phys. Rev. C **48**, 326 (1993).
[22] N. A. Orr *et al.*, in *Proceedings of the 3rd International Conference on Radioactive Nuclear Beams, East Lansing, Michigan,* edited by D. J. Morrissey (Editions Frontieres, Gif-sur-Yvette Cedex, France, 1993), p. 389.
[23] T. Kobayashi, in *Proceedings of the 3rd International Conference on Radioactive Nuclear Beams* (Ref. [22]), p. 169.
[24] G. A. Souliotis *et al.*, Phys. Rev. C **46**, 1383 (1992).
[25] H. Sagawa, B. A. Brown, and H. Esbensen, Phys. Lett. B **309**, 1 (1993).
[26] T. Nakamura *et al.*, Phys. Lett. B **331**, 296 (1994).
[27] B. M. Sherrill *et al.*, Nucl. Instrum. Methods Phys. Res., Sect. B **70**, 298 (1992).
[28] W. A. Friedman, Phys. Rev. C **27**, 569 (1983).
[29] K. Riisager, in *Proceedings of the 3rd International Conference on Radioactive Nuclear Beams* (Ref. [22]), p. 281; private communication.
[30] J. H. Kelley and Sam M. Austin, NSCL Annual Report No. 90, 1993.
[31] H. Esbensen (private communication).